Dynamics of sodium-doped polyacetylene

A. J. Dianoux
Institut Laue-Langevin, 156X, 38042 Grenoble Cedex, France

G. R. Kneller[a)]
IBM France, 68-76 Quai de la Rapée, F-75012 Paris, France and Section de Biophysique des Protéines et des Membranes, Département de Biologie Cellulaire et Moléculaire, CEA, Centre d'Etudes Saclay, 91191 Gif-sur-Yvette Cedex, France

J. L. Sauvajol
Groupe de Dynamique des Phases Condensées, Université Montpellier II, Montpellier Cedex, France

J. C. Smith
Section de Biophysique des Protéines et des Membranes, Département de Biologie Cellulaire et Moléculaire, CEA, Centre d'Etudes Saclay, 91191 Gif-sur-Yvette Cedex, France

(Received 12 January 1994; accepted 22 March 1994)

The low-frequency dynamics (<20 meV) of pure and sodium-doped *trans* polyacetylene are investigated using a combination of incoherent neutron scattering spectroscopy and molecular dynamics simulations. The simulations are performed using a molecular mechanics potential function and including explicitly the three-dimensional crystal environments of the molecules. Both the experiments and the simulations indicate that doping results in a marked change in the vibrational density of states of the polyene chains in the direction perpendicular to the chain axes, a broad minimum appearing at ~16 meV. This spectral region is dominated by intramolecular torsional displacements. The results also suggest that the mean-square displacements of the polyacetylene atoms become more isotropic on doping. The contributions of various rigid-body motions to the simulation-derived mean-square displacements and vibrations are described.

I. INTRODUCTION

The conjugated polyene, polyacetylene, exhibits metallic levels of conductivity when chemically doped.[1,2] The spectacular increase of the conductivity on doping is due mainly to changes in the electronic structure of the polymer backbone. Models of the conduction have been proposed in which charges added to the polyene bring about the formation of charged solitons in polymers with degenerate ground states (such as *trans* polyacetylene) and polarons and/or bipolarons in polymers with nondegenerate ground states (such as *cis* polyacetylene).[3] Solitons and polarons are low-energy excitations involving strong coupling between the electronic and nuclear degrees of freedom.

As a first approximation the conduction can be considered as one-dimensional, proceeding along the conjugated chains. However, a knowledge of the three-dimensional interactions in the crystal is expected to be necessary for a complete description of the conduction, and may strongly influence the conduction rates. A characterization of the ground state dynamics of the polyacetylene and dopant nuclei in the directions parallel and perpendicular to the chains will bring useful information in this regard. The vibrational modes dominating the atomic mean-square displacements are those at low frequencies ($\lesssim$20 meV=30.4 rad ps^{-1}). These modes are accessible experimentally using incoherent inelastic neutron scattering spectroscopy.[4] Neutron scattering is particularly suited to the characterization of low-frequency vibrations as the intensity of scattering by a vibrational mode is proportional to its amplitude. Due to the large incoherent scattering cross section of hydrogen, hydrogen scattering dominates the spectra measured from pure and doped polyacetylene. The hydrogen-weighted vibrational density of states, $G(\omega)$ (where ω is the frequency) can be extracted from the scattering data.

Vibrations in the range <20 meV correspond to picosecond time-scale oscillations that can be examined in detail using the molecular dynamics technique. By calculating $G(\omega)$ from the simulations and comparing with neutron scattering experiments information on the accuracy of the simulation can be obtained. When agreement with experiment is seen the nature of the vibrations detected experimentally can be examined by decomposing the simulated atomic dynamics. This approach has been used to describe picosecond time-scale dynamics in molecular crystals,[5] methylene chloride,[6] proteins[7] and, in a recent paper, pure polyacetylene.[8] In pure polyacetylene the experimentally-derived $G(\omega)$ was found to be highly anisotropic and to vary significantly with the conformation of the molecules, *cis* or *trans*.[9,10] In the recent simulation work the anisotropy and conformation dependence of the $G(\omega)$ observed experimentally were mostly well reproduced.[8] The simulation trajectories were further analyzed so as to determine the dynamical contributions to the observed spectra. The lowest-frequency vibrations parallel to the chain axes, at 1.5 meV in the *cis* system and 4 meV in the *trans* system, were found to result from whole-molecule rigid-body translations, invariant with chain length. Conversely, the low-frequency intramolecular vibrations were found to be weakly dependent on chain conformation but to vary strongly with the chain length.

The success of the molecular dynamics neutron scatter-

[a)]Preset address: Institut für Theoretische Physik A, RWTH Aachen, Templegraben 55, D-52056 Aachen, Germany.

 0021-9606/94/101(1)/634/11/$6.00

ing analysis of the dynamics of the pure polyacetylene system suggests that the combined approach should be extended to investigate the dynamics of doped polyacetylene. In the present paper we present experimental and simulation-derived data on *trans* polyacetylene doped with 12.5% at. wt. sodium. A marked change in the experimental $G(\omega)$ is found on doping. This involves the appearance of a broad minimum at ~16 meV in the directions perpendicular to the chain axes. Molecular dynamics simulations using an equivalent model system are described. In the model system complete ionization of the sodium atoms and uniform distribution of the excess negative charges over the polyene carbon atoms are assumed. The resulting parallel and perpendicular $G(\omega)$ are found to reproduce well the observed experimental spectra and the differences resulting from doping.

The paper is organized as follows. In Sec. II we describe briefly the simulation and analysis procedure. In Sec. III the results are presented. After some preliminary energy calculations the anisotropic simulation-derived time-dependent mean-square displacements, $\Delta R^2(t)$ of the carbon, hydrogen, and sodium atoms are presented. $G(\omega)$ is calculated in the perpendicular and parallel chain directions and compared with the corresponding experimental quantities. A decomposition of the molecular dynamics trajectory in terms of rigid-body motions of the polyacetylene chains and columns of sodium ions is performed and the contribution of these motions to $G(\omega)$ and $\Delta R^2(t)$ determined. These quantities are compared with those calculated from the simulations of the pure *trans* polyacetylene. The paper ends with a concluding discussion.

II. METHODS

A. Experiment

The experimental vibrational densities of states were obtained from incoherent inelastic neutron scattering intensities on stretch-oriented *trans* polyacetylene doped to 12.5% at. wt. with sodium. The experiments were performed on the MiBeMol time-of-flight spectrometer at Saclay. Details will be published elsewhere.[11]

B. Molecular dynamics

The molecular dynamics simulations were performed with the program CHARMM (Ref. 12) running on an Alliant VFX 80 and an IBM RISC 6000 workstation at Saclay. The simulation methodology follows that described in Ref. 8 in which pure *trans* polyacetylene was simulated. Results from the pure $(CH)_x$ simulation are recalled in the present paper for comparison with those obtained in the doped polymer simulations. In the following paragraphs we describe in detail the model system derived to represent Na-doped $(CH)_x$.

The potential energy as a function of the relative nuclear coordinates is represented using a molecular mechanics type energy function. The function is given in Eq. (1),

$$V=\sum_{\text{bonds}} k_b(b-b_0)^2+\sum_{\text{angles}} k_\theta(\theta-\theta_0)^2 + \sum_{\text{dihedrals}} k_\phi[1+\cos(n\phi-\delta)]+\sum_{\text{impropers}} k_\omega(\omega-\omega_0)^2 + \sum_{i,j} 4\epsilon_{ij}\left[\left(\frac{\sigma_{ij}}{r_{ij}}\right)^{12}-\left(\frac{\sigma_{ij}}{r_{ij}}\right)^{6}\right]+\sum_{i,j}\frac{1}{4\pi\epsilon}\frac{q_iq_j}{r_{ij}}. \quad (1)$$

The force field includes *bonded interactions*, comprising bond stretches, bond angle bends, improper dihedral and proper dihedral angle contributions, and nonbonded interactions between pairs (i,j) of atoms. In Eq. (1), b, θ, ϕ, and ω are the bond lengths, angles, dihedrals, and improper torsions at any given configuration and b_0, θ_0, ω_0 are the reference values for these properties; the associated force constants are k_b, k_θ, k_ϕ, and k_ω. For the intrinsic torsions n is the symmetry number of the rotor and δ is the phase angle. The improper dihedral contributions are used to represent out-of-plane deformations of the sp_2 groups.

The model used treats all atoms in the system explicitly. The nonbonded interactions are included for atoms on different molecules and for atoms on the same molecule separated by three or more bonds. The nonbonded interactions between pairs of atoms i,j consist of a Lennard-Jones van der Waals term, with well-depth $\sigma_{i,j}$ and van der Waals radius $\epsilon_{i,j}$ and an electrostatic interaction between partial charges q_i,q_j. The dielectric constant, $\epsilon=\epsilon_0\cdot\epsilon_r$ was set to $\epsilon=\epsilon_0$, i.e., $\epsilon_r=1$.

Polyacetylene consists of alternating short, C=C and long, C–C bonds. There has been considerable discussion as to the origin of the bond alternation. Simplified models describe the appearance of bond alternation as a symmetry-breaking "dimerization" of successive carbon sites, resulting from a Peierls-type instability of the hypothetical system in which carbon–carbon bond lengths are equal.[3,13,14] Peierls distortion is driven by electron–phonon coupling. However, it has been suggested from calculations including explicit electron–electron interactions that the bond alternation is due principally to these electron correlation terms.[15,16] Infrared conductivity experiments have provided indirect evidence that that the alternating short C=C and long C–C bonds persist to the highest dopant levels.[18–20] For our simulations of the doped system the bond alternation adopted in the simulations of the pure $(CH)_x$ molecules was kept. With the exception of the partial charges, all the potential function parameters used in the simulations of pure polyacetylene, listed in the Appendix of Ref. 8, were adopted for the simulations of the doped system.

The potential energy function used for the sodium ion: polyacetylene and sodium ion:sodium ion interactions consists of electrostatic and van der Waals terms. The van der Waals parameters ($\epsilon=-0.0448$ kcal/mol and $R_{\min}/2=1.532$ Å) were taken from fitting to *ab initio* quantum chemical calculations of sodium:organic group interactions.[21] Nuclear magnetic resonance measurements on sodium-doped polyacetylene indicate that the sodium resonance is unshifted with respect to standard ionic reference compounds.[22] Therefore, we assume that the sodium atoms are completely ionized and assign a charge of +1 electron unit to each of them.

The question arises of how to distribute the excess electronic charge over the polyacetylene chains. At low doping levels it has been suggested that the charges localize to form nonlinear configurations (solitons).[3] There is evidence that doping reversibly transforms the electronic structure of the polymer from a semiconductor to a metal at high doping levels such as that considered here.[3] The transition may involve the formation of a degenerate Fermi sea with no significant accompanying structural change.[23] In view of the high doping level considered in the present calculations we have assumed that the excess electronic charge is distributed evenly over the polyacetylene carbon atoms. However, we note that there is still uncertainty as to what the charge distribution should be and that evidence for an uneven distribution of the negative charge has been provided from semiempirical quantum chemical calculations on negatively charged polyene anions.[24] The potential function [Eq. (1)] uses point charge representations of the charges, centered at the nuclei. We uniformly distribute the excess negative charge over the carbon atom point charges in the system. Thus, the charge on each carbon is -0.225 electron units, 0.125 electron units more negative than that used in the simulations of the pure system. The charge on the hydrogen atoms was assumed to be identical to that used for the pure system, i.e., $+0.100$ electron units.

Polyacetylene is frequently idealized as a collection of infinite, highly conjugated one-dimensional chains. However, near-infrared photoluminesence experiments on thermally-isomerized polyacetylene[25] have provided evidence that *trans* $(CH)_x$ is best viewed as a three-dimensional ensemble of short, conjugated segments that are bounded and interconnected by defects and crosslinks. The experiments were interpreted as indicating that mean segment lengths are probably less than 13 CH=CH units (26 carbons). In the present simulations a chain length of 64 carbons was adopted, in approximate accord with the conjugation lengths derived in Ref. 25.

The polyacetylene systems were simulated including the full crystal environment using classical molecular dynamics and periodic boundary conditions. The use of periodic boundary conditions suppresses vibrations with wavelengths longer than the box sides. The primary box for the doped-system simulations consisted of 12 polyacetylene $(CH)_{64}$ molecules and 96 sodium ions, i.e., 1 sodium ion per 8 CH groups. The dimensions of the primary box, calculated from x-ray diffraction results,[26] were $x=15.13$ Å, $y=13.10$ Å, $z=81.31$ Å. To represent in an approximate way the environment experienced by the terminal atoms a weak harmonic constraint was applied to the terminal hydrogen atoms of the polyacetylene, identical to that described in Ref. 8.

Nonbonded interactions were truncated using a spherical cutoff of 11 Å with a cubic switching smoothing function applied between 9 and 11 Å. This cutoff is longer than half the box length, indicating that the minimum image convention is not adopted; in the directions perpendicular to the chain axes a given atom may interact with another atom and its image. As the system is crystalline this is not expected to introduce serious artefacts. Moreover, the longer cutoff reduces unphysical electrostatic truncation forces. In the parallel direction the cutoff is much shorter than half the box length (the length is 81.31 Å). This is convenient as the experimental systems are not periodic (they are disordered) in this direction. The nonperiodicity in the parallel direction suggests that the use of an Ewald summation of electrostatic energies would introduce artefacts, particularly in the sodium–sodium interactions. Ewald summation was not used in the present simulation.

A dynamical snapshot of the simulation primary box is shown in Fig. 1(a). Initial positions for the dopant were chosen by uniformly distributing 24 sodium ions inside each of the triangular channels formed by three adjacent $(CH)_{64}$ molecules. The starting configuration for the simulations was obtained by minimization of the potential energy of the crystal with fixed unit cell dimensions. Simulations were performed in the microcanonical ensemble with an integration timestep of 1 fs and the bond lengths involving hydrogen atoms were constrained with the SHAKE algorithm.[27] Each simulation consisted of three phases; a 2000 step Langevin dynamics heating phase, an equilibration run of 2000 steps with occasional velocity scaling to stabilize the temperature, and a production phase of 82 ps without velocity scaling. The average temperature during the simulation was 303 K with a rms fluctuation of 5 K. The production run configurations were dumped to disk every 10 steps.

Molecular dynamics simulations of pure and potassium-doped polyacetylene have been reported recently.[28,29] The methodology used in these simulations has several differences from that employed here. One particularly significant difference is the absence of torsional terms in the energy function. The low-frequency dynamics of interest here involves displacements of primarily torsional degrees of freedom. As the torsional barriers of both the C–C bonds and the C=C bonds are high (7 and 60 kcal/mol, respectively, in the present model) their omission will lead to a poor model of the the low-frequency dynamics of the polyacetylene chains. The 7 kcal/mol intrinsic torsional contribution to the *gauche/trans* potential barrier is sufficiently high to prevent C–C torsional transitions in the present simulation.

C. Analysis

Time-dependent mean-square displacements, $\Delta R^2(t)=\langle[R(t)-R(0)]^2\rangle$ and vibrational densities-of-states, $G(\omega)$ were derived from the production dynamics positions and velocities. $G(\omega)$ is the Fourier-transform of the velocity autocorrelation function, i.e.,

$$G(\omega)=\frac{1}{N}\sum_{\alpha}\frac{1}{2\pi}\int_{-\infty}^{\infty}dt e^{-i\omega t}\langle \mathbf{v}_\alpha(0)\mathbf{v}_\alpha(t)\rangle, \tag{2}$$

where $\langle \mathbf{v}_\alpha(0)\mathbf{v}_\alpha(t)\rangle$ is the autocorrelation function of the velocities, $\mathbf{v}_\alpha(t)$ of atom α ($\alpha=1,...,N$). The full-width at half-maximum resolution of the simulation-derived densities of states is ~0.5 meV. The simulation lengths permitted the reliable determination of the correlation functions over a time period of 10 ps for the pure system and 20 ps for the doped system. $\Delta R^2(t)$ and $G(\omega)$ were calculated in the directions perpendicular and parallel to the chain axes.

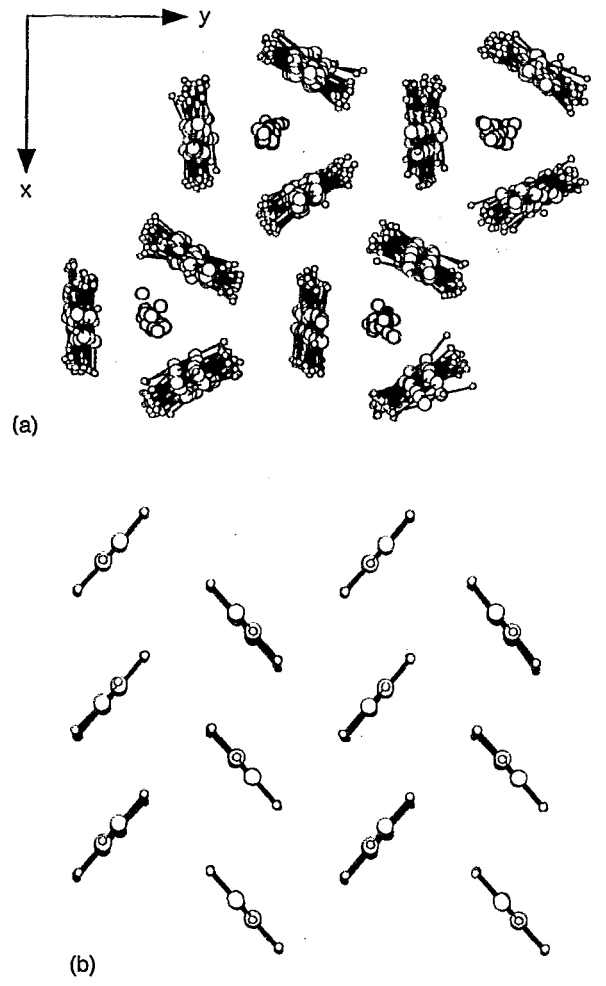

FIG. 1. (a) Snapshot of the simulation primary box after 16.5 ps of production dynamics. This view is approximately in the xy plane. (b) Energy minimized structure of primary simulation box of dedoped polyacetylene. The minimization was performed with primary box dimensions corresponding to the experimental pure *trans* structure and was pursued to a rms energy gradient <0.1 kcal/mol Å.

Rigid body trajectories were obtained by fitting reference structures from the energy-minimized starting configuration onto each of the molecules in the primary box for each molecular dynamics time frame and storing the Cartesian coordinates of the fitted atom positions and the parameters of the fit describing the translational and rotational degrees of freedom. A general method for the optimal superposition of molecular structures was used for the fits.[30] For more details see Refs. 5 and 30.

III. RESULTS

In what follows we first consider some energetic aspects of the $(CH)_x$ chains in the doped configuration with and without the presence of sodium ions. Following this the dynamical results are given. The time-dependent mean-square displacements of the carbon atoms, hydrogen atoms, and sodium ions are calculated from simulations of pure $(CH)_{64}$ and the sodium-doped form. The polyacetylene atom $\Delta R^2(t)s$ are dominated by low-frequency vibrations involving rigid-molecule motions and coupled displacements of torsional degrees of freedom. The frequencies involved are analysed via the vibrational frequency distribution, $G(\omega)$. $G(\omega)$ for the hydrogen atoms is directly compared with results from neutron scattering experiments. Of particular interest are the anisotropy of the calculated quantities and the comparison of the polyacetylene chain motions in the presence and absence of dopant.

A. Energy calculations

A basic question concerns the results given by the present model and potential function for various interaction energies involving the sodium ions. In the energy-minimized starting structure the interaction energy between a sodium ion and the $(CH)_{64}$ chains in the primary simulation box is -286 kcal/mol of which $+9$ kcal/mol is van der Waals energy and -295 kcal/mol is electrostatic. Of the electrostatic contribution -263 kcal/mol arises from interactions with nine close carbon atoms, three on each chain. The three carbons on each chain interact at distances of 2.66, 2.40, and 2.61 Å from the sodium. The sodium interacts with the other sodium ions in the primary box with an electrostatic energy of 197 kcal/mol.

The behavior in the model of the polyacetylene chains on the removal of sodium ions is of interest. To investigate this energy minimizations were performed on chains in the triangular geometry of the doped system [e.g., Fig. 1(a)] with both the sodium ions and the excess negative charge on the $(CH)_{64}$ removed, and with the primary box dimensions fixed at those found experimentally for the pure *trans* system.[31–33] The geometry resulting from the minimization is shown in Fig. 1(b). The pure *trans*, herringbone structure has been recovered. The setting angle (the angle between the chain plane and the y axis) is 50°. This can be compared to values obtained by diffraction experiments of 51° (Ref. 32) and 55°.[33] The potential energy of the minimized system is identical to that obtained by directly minimizing the experimental *trans* structure. Thus, energy minimization of the doped system on removal of sodium results in a structural transition from the triangular (doped) to herringbone (pure *trans*) geometry. This indicates that interactions between $(CH)_x$ chains do not present energy barriers to the doped-to-pure structural transition.

The energy decrease per $(CH)_{64}$ molecule on energy minimization is 153 kcal/mol of which 145 kcal/mol is van der Waals energy; the transition is therefore essentially driven by van der Waals (packing) forces. To further examine this effect another energy minimization was performed but with the primary box parameters of the doped system. In this case the *trans* structure was only partially recovered (not shown) as the van der Waals interactions between the primary box and its images were not optimal. This indicates that the optimized structure is sensitive to the box parameters.

B. Mean square displacements

We now investigate the time-dependent atomic mean-square displacements $\Delta R^2(t)$, derived from the production phases of the molecular dynamics simulations of the pure and doped systems.

1. Pure polyactylene

In Figs. 2 are presented the ΔR^2 for the hydrogens and carbons in the pure $(CH)_{64}$ simulation. The correlation functions manifest a short time-scale (<1 ps) rise due to dephasing of the high-frequency vibrations. After this the correlation function in the parallel direction converges to a plateau value modulated by low-frequency oscillations. An approximate convergence is seen also in the perpendicular direction although motions with longer characteristic times are present. The approximate convergence of the mean-square displacements indicates that no significant diffusive behavior is present on the time scale considered and the motion of the chains is essentially vibrational. This is consistent with the absence of detectable quasielastic neutron scattering in the experiments.[9] The mean value of ΔR^2 after the vibrational dephasing (the "long-time" amplitude) is markedly anisotropic, the ratio of the perpendicular to parallel mean-square displacements, $\Delta R_\perp^2/\Delta R_\parallel^2$ is ~3 for both the carbons and hydrogens. This anisotropy arises in part from the geometry of the soft degrees of freedom of the polyacetylene chains. These are the C–C torsions that, in a perfectly oriented chain, have components in only the perpendicular directions. The ratio of the hydrogen ΔR^2 to the carbon ΔR^2 is ~1.4 in both the perpendicular and parallel directions. In the perpendicular direction this can again be explained in terms of the geometry of the C–C torsions. However, in the parallel direction the increased hydrogen ΔR^2 implies the presence of significant displacements of harder degrees of freedom and/or chain axis reorientations. Low-frequency vibrations are clearly visible in $\Delta R_\parallel^2$. These have a period of ~1 ps (frequency ~4 meV) and an initial amplitude of ~0.03 Å^2.

The contribution to the atomic displacements from the polyacetylene molecules acting as rigid bodies without internal motion was calculated by fitting an energy-minimized $(CH)_{64}$ molecule to each simulation timeframe for each molecule in the primary box. In Fig. 3 are presented ΔR^2 for the motion of the center-of-mass of the rigid chains and ΔR^2 averaged over the atoms in the fitted rigid-molecule trajectories. The center-of-mass ΔR^2 contains only translational rigid-chain dynamics. The atom-averaged rigid-chain $\Delta R_\parallel^2$ is strictly identical to that of the center-of-mass but $\Delta R_\perp^2$ contains a contribution from rotational rigid-chain motion.

A comparison of Figs. 2 and 3 indicates that about half of $\Delta R_\parallel^2$ can be described in terms of rigid-body motion of the chains. The 4 meV (6 rad ps^{-1}) oscillation visible in the full $\Delta R_\parallel^2$ in Fig. 2 is identified as a rigid-molecule translational vibration. This vibration makes a large contribution to the rigid-molecule $\Delta R_\parallel^2$. The comparison of Figs. 2 and 3 indicates that the proportion of $\Delta R_\perp^2$ that can be attributed to rigid-molecule displacements is smaller than for $\Delta R_\parallel^2$. The major contribution to the rigid-molecule $\Delta R_\perp^2$ at most times is from rotational motion. The long time-scale variations visible in $\Delta R_\perp^2$ in Fig. 2 are attributed to rigid-molecule motion perpendicular to the chain axes.

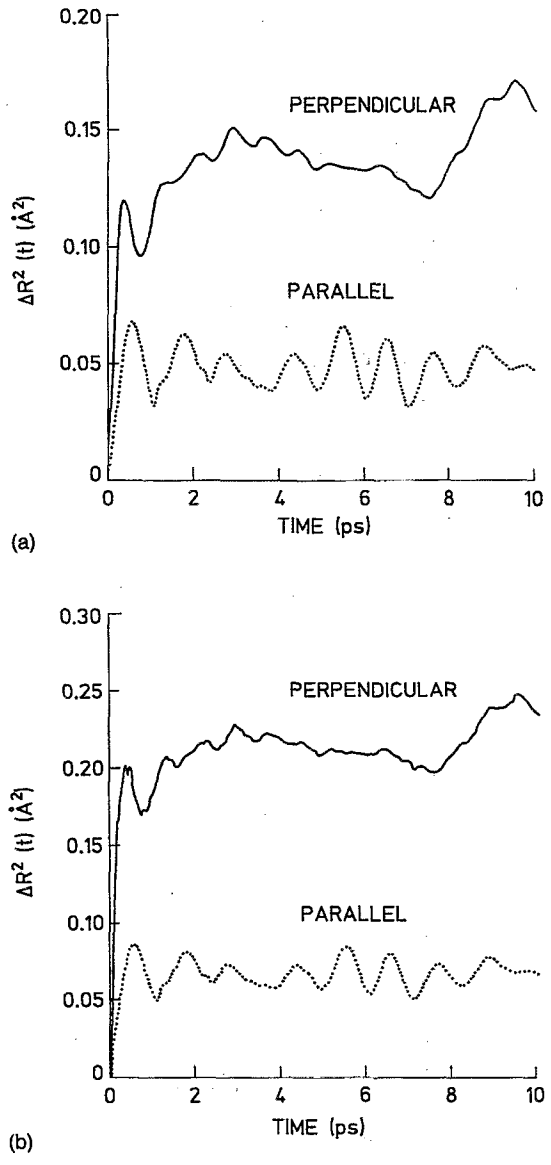

FIG. 2. Time-dependent mean-square displacements, $\Delta R^2(t)$ per atom for pure polyacetylene (a) carbons (b) hydrogens.

2. Na-doped polyacetylene

We now examine the dynamics of the Na-doped polyacetylene chains and compare with the results obtained for the pure *trans* system. In Fig. 4 are shown $\Delta R_\perp^2$ and $\Delta R_\parallel^2$ for the carbon and hydrogen atoms from the Na-doped *trans*-$(CH)_{64}$ simulation. The most striking difference from the undoped system is that the anisotropy in ΔR^2 is much less marked; the average long-time $\Delta R_\parallel^2$ has increased from ~0.05 Å^2 in the undoped case to ~0.20 Å^2 in the doped system such that it is similar in magnitude to that of $\Delta R_\perp^2$. The values of the average long-time hydrogen and carbon

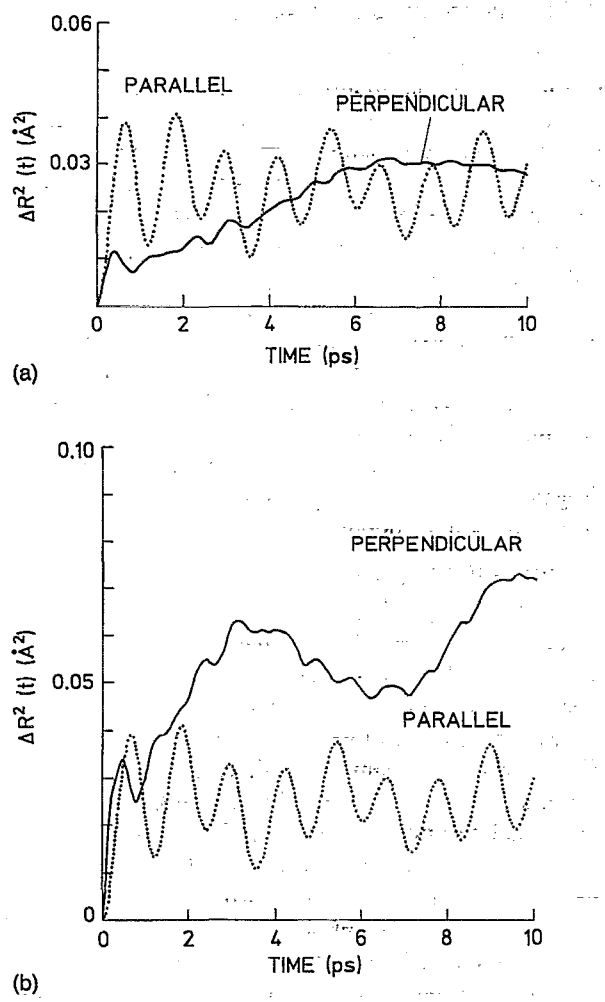

FIG. 3. Rigid-molecule component of $\Delta R^2(t)$ for pure polyacetylene (a) for the center-of-mass of the rigid molecule; (b) averaged over the atoms of the rigid molecule.

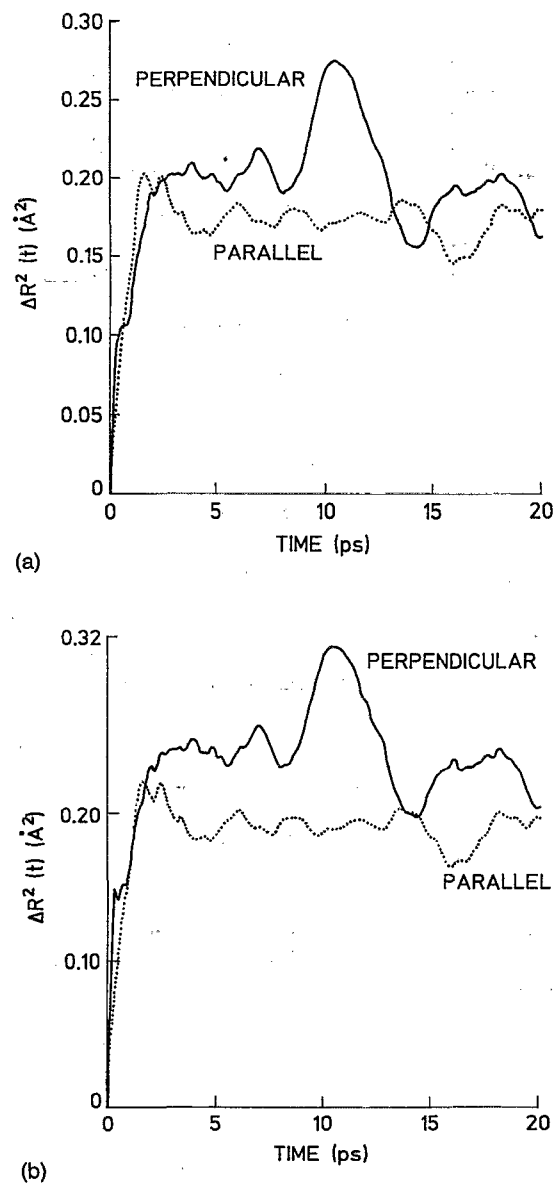

FIG. 4. Time-dependent mean-square displacements, $\Delta R^2(t)$ for Na-doped polyacetylene (a) carbons (b) hydrogens.

$\Delta R_\perp^2$s are slightly increased in the presence of sodium. The ratio of the hydrogen ΔR^2 to that of the carbons is ~1.2, compared with ~1.4 in the undoped case.

In Fig. 5 are presented the ΔR^2s obtained from rigid-molecule fits to the trajectories of the polyacetylene atoms. The rigid-molecule translational $\Delta R_\parallel^2$ has increased markedly from ~0.02 Å^2 in the undoped case to ~0.15 Å^2 in the doped system where it contributes ~75% of the full trajectory $\Delta R_\parallel^2$. The form of the rigid-molecule $\Delta R_\perp^2$ resembles closely that in the undoped case although the amplitude is reduced. As in the undoped case $\Delta R_\perp^2$ for the atom-averaged rigid-molecule motion is reduced more than twofold compared to $\Delta R_\perp^2$ derived from the full trajectories; a major proportion of $\Delta R_\perp^2$ arises from non rigid-molecule motion. However, very low-frequency oscillations (~0.5 meV frequency) are clearly present in the rigid-molecule $\Delta R_\perp^2$ and are visible as components of the full trajectory $\Delta R_\perp^2$.

Figure 1 indicates that the sodium ions stay more or less in the center of the channels formed by 3 adjacent $(CH)_{64}$ molecules. The $\Delta R_\parallel^2$ and $\Delta R_\perp^2$ for the sodium ions are presented in Fig. 6. Whereas the average long-time ΔR^2 for the $(CH)_{64}$ molecules is close to isotropic this is not the case for the sodium ions; $\Delta R_\parallel^2$ is about half as large as $\Delta R_\perp^2$. There is strictly no diffusive or longer time scale oscillatory motion of the sodium ions in the parallel direction. The form of $\Delta R_\perp^2$ of the sodium ions resembles that of the $(CH)_{64}$ atoms, suggesting that they are correlated in the perpendicular direction. This correlation and the existence of a plateau in $\Delta R_\perp^2$ indicates that the sodium ions are constrained by the strong electrostatic interactions with the polyacetylene chain carbons that are detailed in Sec. III A.

Rigid-body fits were performed of columns of 24 sodium ions on the full trajectories; the resulting mean-square displacements are presented in Fig. 7. $\Delta R_\parallel^2$ is clearly very well described by the rigid column displacements whereas $\Delta R_\perp^2$ contains a significant contribution (~40%) due to nonrigid-column motion.

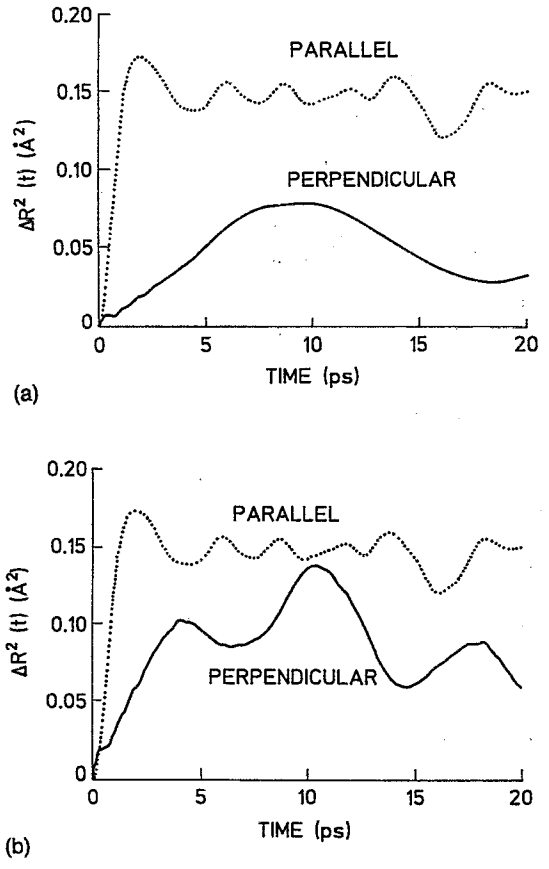

FIG. 5. Rigid-molecule component of $\Delta R^2(t)$ for Na-doped polyacetylene (a) for the center-of-mass of the rigid molecule; (b) averaged over the atoms of the rigid molecule.

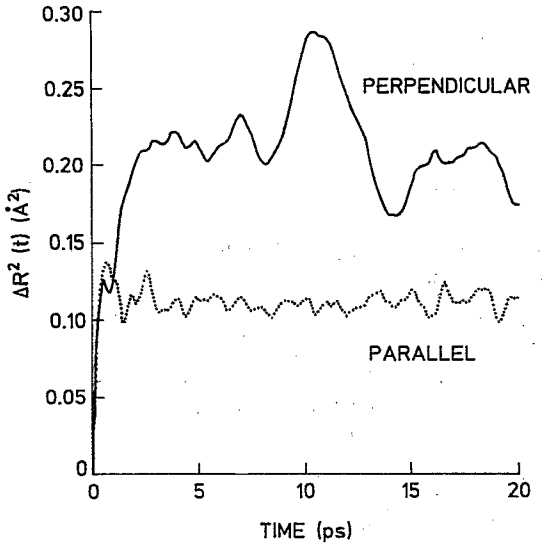

FIG. 6. Time-dependent mean-square displacements, $\Delta R^2(t)$ for the sodium ions.

C. Vibrational density of states

The results presented in the previous section indicate that the major contribution to the ps time-scale mean-square displacements arises from vibrational motion. To examine in further detail the dynamics concerned requires a determination of the vibrational frequencies involved. Since the large-amplitude vibrations determine $\Delta R^2(t)$, and these are of low-frequency, the low-frequency density of vibrational states, $G(\omega)$ is the relevant physical quantity. In this section we present simulation-derived densities of states and compare them with corresponding quantities derived from incoherent inelastic neutron scattering experiments[9,10] on pure and doped polyacetylene. The previous work demonstrated that the simulations are capable of reproducing the anisotropy and conformation-dependence of the low-frequency hydrogen $G(\omega)$ for pure polyacetylene.[8] Here we examine the effect on $G(\omega)$ of doping *trans* polyacetylene.

1. Pure polyacetylene

In Fig. 8(a) we recall the low-frequency region of the experimentally-derived $G_\parallel$ and $G_\perp$ spectra for pure *trans*-$(CH)_x$. These data were collected on the IN6 spectrometer at the Institut Laue-Langevin. The counting statistical error is of the order of the thickness of the lines on Fig. 8(a). The corresponding simulation-derived densities of states are presented in Fig. 8(b), convoluted with the experimental instrumental resolution function and with the crystal mosaic spread taken into account. The simulation-derived pure *trans* spectrum is in good agreement with the experimental $G(\omega)$. A detailed analysis of these vibrations was presented in the previous paper.[8] Rigid molecule fits showed that the lowest frequency (4 meV) $G_\parallel$ feature is entirely due to rigid-molecule translations whereas the other low-frequency $G_\parallel$ features are internal motions of the chains. $G_\perp$ contains a rigid-molecule component at very low frequencies (~4–12 meV). The major contribution to $G_\perp$ at frequencies >5 meV arises from internal, nonrigid-body motions.

2. Effect of doping

In Fig. 9 are presented the low-frequency spectra of the simulation-derived $G_\parallel$ spectra for *trans*-$(CH)_{64}$ and Na-doped *trans* $(CH)_{64}$. These spectra have not been convoluted

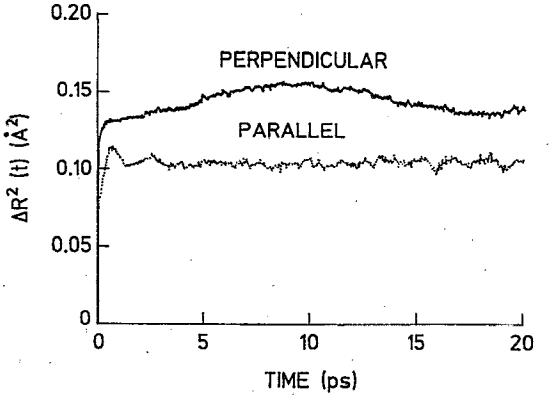

FIG. 7. Rigid-body component of $\Delta R^2(t)$ for sodium ions.

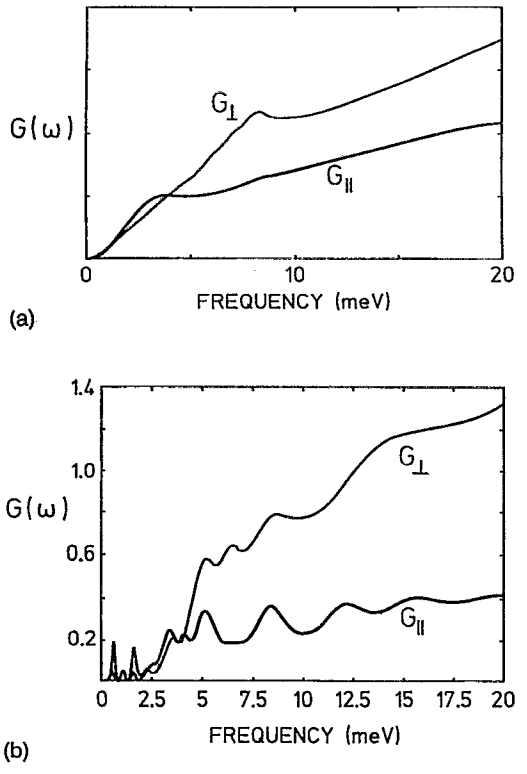

FIG. 8. Low-frequency $G(\omega)$ for pure *trans* polyacetylene. (a) Experimental; (b) simulation.

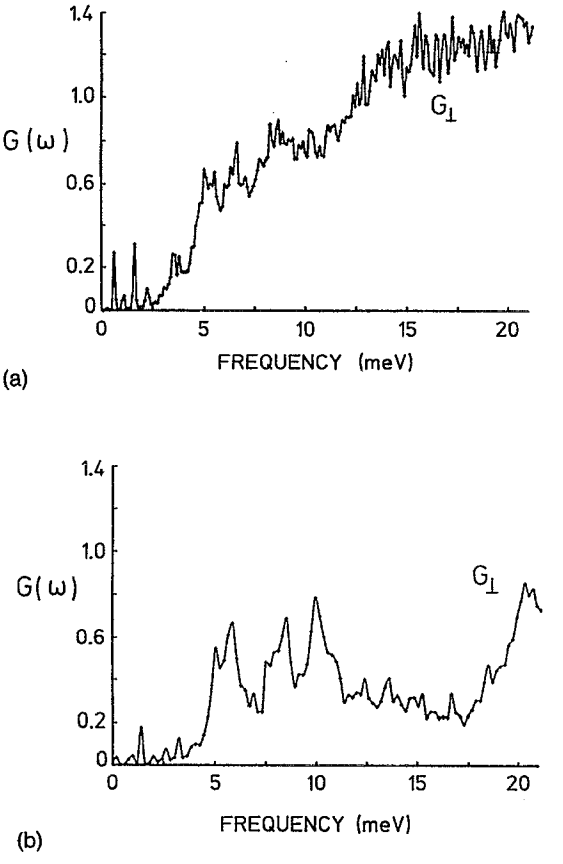

FIG. 10. Low-frequency simulation-derived $G_\perp$ for (a) pure polyacetylene; (b) Na-doped polyacetylene.

with an instrumental resolution function. Some differences between the two spectra are visible. The shoulder at 4 meV in the experimental resolution-broadened $G_\parallel$ of pure *trans*-$(CH)_{64}$ [Fig. 8(a)] is seen in Fig. 9(a) to arise from several vibrations between 2.5 and 4.5 meV. These vibrations shift to low frequencies in the doped system, to between 1 and 3 meV. Rigid-molecule fits indicate that these vibrations are rigid-molecule translations. Their decrease in frequency is consistent with the increased rigid-molecule $\Delta R_\parallel$ in the doped system (Fig. 5). The peak at 5 meV in the undoped system is an intramolecular vibration. It is also shifted to a slightly lower frequency in the doped system. The vibrations at higher frequencies are all unshifted. Normal mode analysis of the isolated chain indicate that they are intramolecular, coupled displacements of primarily the C–C torsional degrees of freedom.[8]

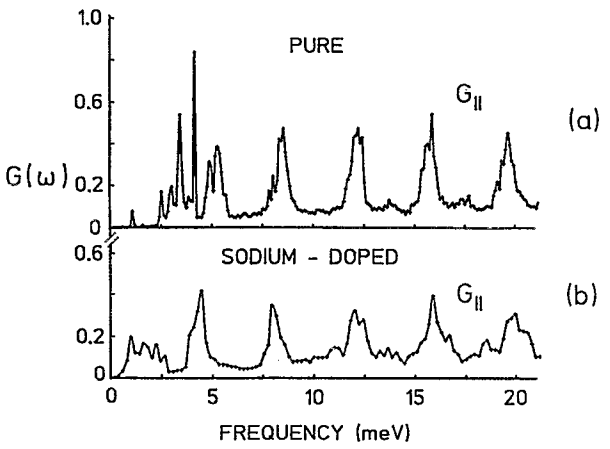

FIG. 9. Low-frequency simulation-derived $G_\parallel$ for (a) pure polyacetylene; (b) Na-doped polyacetylene.

Figure 10 shows the same, low-frequency region of the simulation-derived $G_\perp$ spectra of *trans*$(CH)_{64}$ and Na-doped $(CH)_{64}$. There is a considerable difference in $G_\perp$ between the doped and undoped species. In the pure system the intensity increases steeply from 5 meV to a plateau at ~15–20 meV, whereas in doped $(CH)_{64}$ a broad minimum is present at ~12–18 meV. The corresponding experimental spectra for Na-doped *trans*-$(CH)_x$ are presented in Fig. 11. These data were collected on the MiBeMol instrument at Saclay. This incident neutron flux on this instrument is much lower than that used for the pure $(CH)_x$ experiment. Therefore, the counting statistics for the Na-doped sample are much worse than in Fig. 8(a). Nevertheless, the broad minimum in the $G_\perp$ spectrum at 12–18 meV is clearly present in the experimental data, in accord with the simulation results of Fig. 9(b). In the experimental $G_\parallel$ a weak shoulder is visible at ~3 meV. This shoulder is at ~4 meV in the pure $(CH)_x$ data and suggests that the shift to low frequencies of the rigid-molecule modes seen in the simulations may also be present experimentally.

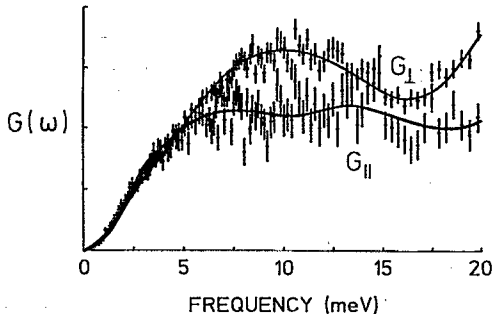

FIG. 11. Experimental $G_{\parallel}$ and $G_{\perp}$ for 12.5% at. wt. sodium-doped polyacetylene.

Vibrations in the polyacetylene chains exist at higher frequencies (>20 meV) and can also be examined by molecular dynamics simulation. These vibrations have been discussed for the pure system.[8] For the doped system high-frequency spectra derived from the simulation have been presented.[34] It is found that the higher-frequency vibrations do not change frequency on doping but that their polarization does change, reflecting a change in the distribution of chain orientations in the doped system.

Figure 12 presents the simulation-derived $G(\omega)$ for the sodium ions in the parallel and perpendicular directions. In both directions low-frequency modes (<18 meV) are present. At higher frequencies the spectra are clearly anisotropic; the $G_{\parallel}$ spectrum has a maximum at ~26 meV and no significant intensity above ~40 meV while the $G_{\perp}$ spectrum has a maximum at somewhat higher frequencies (~38 meV) and extends up to ~70 meV (106 rad ps^{-1}). A rigid-body analysis for columns of sodium ions was performed in a fashion analogous to that for the polyacetylene molecules, i.e., a rigid column of 24 sodium ions inside a channel was fitted to the corresponding full trajectories. The result is shown in Fig. 13; in $G_{\parallel}$ nearly all the features which are seen on Fig. 12 between 1 and 3 meV are due to rigid-body oscillations of the sodium ions inside the channels. This low-frequency motion of the sodium ions occurs in the same frequency range as the rigid-body translation of the polyacetylene chains. $G_{\parallel}$ at frequencies >3 meV consists almost entirely of nonrigid-column vibrations. The rigid-body contribution to $G_{\perp}$ is small.

IV. CONCLUDING DISCUSSION

Molecular dynamics simulations reported previously reproduce well both the anisotropy and conformation-dependence (*cis* or *trans*) of the experimental low-frequency vibrational density of states of pure polyacetylene.[8] The major results of the present work are that corresponding experimental spectrum of Na-doped polyacetylene is markedly different to the undoped system in the direction perpendicular to the chain axes and that this difference is also seen in molecular dynamics simulations of the crystalline system. Although the potential energy function used in the simulations is empirical it has not been adjusted to fit the experimental data presented here. The agreement with experiment obtained with the present potential function attests to its ability to reproduce the basic characteristics of the dynamics of the polyacetylene chains in these systems.

The simulations suggest that there is also a change in the mean-square displacements on doping. Whereas in the pure *trans* system ΔR^2 is very anisotropic this is not the case in the doped system. The effect of doping is to increase by a factor of ~3 the rigid-molecule ΔR^2 in the direction parallel to the chain axes. A reduction in the corresponding rigid-

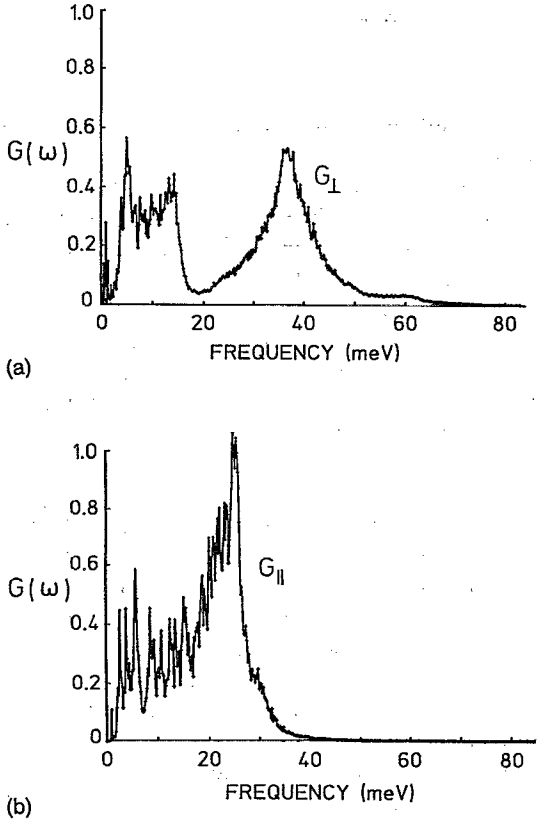

FIG. 12. Simulation-derived $G(\omega)$ for the sodium ions. (a) $G_{\perp}$; (b) $G_{\parallel}$.

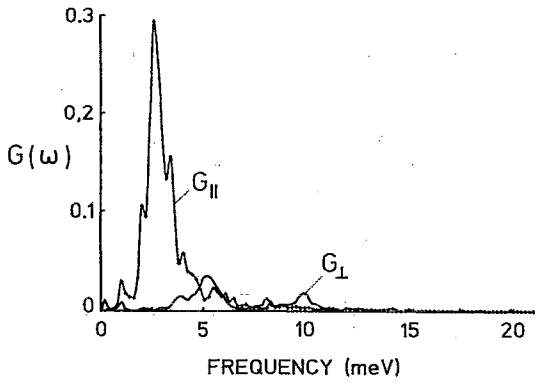

FIG. 13. Low-frequency simulation-derived sodium ion rigid-body $G(\omega)$. (a) $G_{\perp}$; (b) $G_{\parallel}$.

molecule vibrational frequencies in the parallel direction was found. There is a suggestion from the experimental $G(\omega)$ that a similar frequency shift may be present; clarification of this will require the collection of neutron data with improved counting statistics. Improved counting statistics will be obtainable with a more powerful neutron source than the one at Saclay. This may also enable a more direct measurement of the anisotropy in ΔR^2 via the scattering wave vector dependence of the elastic incoherent scattering.

Whereas the mean-square displacements of the atoms in the chains are fairly isotropic in the doped system simulation, those of the sodium ions are not. In the perpendicular direction the sodium ion displacements are coupled to the chain motion; in the parallel direction the ion displacements are reduced and the ions vibrate without any long time-scale oscillations or diffusive motion. The sodium ion dynamics have not yet been investigated experimentally. A spectroscopic technique such as synchrotron far-infrared spectroscopy may prove useful in investigating their low-frequency vibrations; the complementarity of this approach with neutron scattering for the determination of low-frequency vibrations in macromolecules has been demonstrated recently.[35]

An important question concerns the effect of the large-amplitude, low-frequency dynamics investigated here on the conduction properties. A much-discussed, possible conduction mechanism involves the propagation of solitons along the chain as nonlinear excitations of charge-carrying lattice defects.[3] However, there has been debate on whether the explicit inclusion of electron–electron interactions still results in solitons as the main charge carriers (see, e.g., Refs. 36,37,38). In simplified, tight-binding models that incorporate the soliton idea (e.g., the Su, Schreiffer, Heeger model[13,14]) electron–phonon coupling is represented using terms containing only explicit nearest neighbor C...C interactions along the chain. These degrees of freedom correspond to C–C and C=C bond length terms in the present potential function; their variation does not contribute significantly to the low-frequency motions described here. However, the possibility that electron–phonon coupling may not be confined to bond length fluctuations and that other, lower-frequency fluctuations may be coupled to the electron transfer has recently been examined.[39] The possible influence of sound waves on diffusive properties of solitons has also been discussed.[3]

Tight binding theory implies weak interchain coupling and the system is regarded as quasi-one-dimensional. However, it has been suggested that, at least at high dopant levels, interchain coupling, scattering of charge carriers by phonons and structural disorder are all potentially of comparable importance to the simplified electron–phonon interaction considered in the tight binding models. That interchain interactions might play an important role in the conduction process has been suggested theoretically[40] and on the basis of near-infrared photoluminescence experiments.[25] In Ref. 25 the main interchain conduction effect was suggested to be due to crosslinking, an effect not explicitly included in the present model. The influence of chain endings and other conjugation breaks on the stability of large polarons has been investigated[41] and the effect of interchain electron hopping on polaron structure has been examined.[42]

Whether the low-frequency dynamics investigated here has a major effect on the conduction properties of Na-doped polyacetylene remains to be seen. However, it is clear that an understanding of the structural and dynamical properties of the three-dimensional system will be necessary for an improved understanding of the conduction process. This will require a combination of quantum chemical calculations, classical mechanical simulations and experiments. The simulations reported here can be improved in several ways. An improved parameterization of the molecular mechanics empirical potential can be made by using results from quantum chemical calculations on the polyene charge distribution and on the sodium:polyene interactions. Molecular dynamics simulations using an energy calculated directly using quantum chemical methods are becoming feasible and could in principle be employed to investigate dynamical charge fluctuations in the system.[43] In the present model the C–C and C=C torsional barriers used in the undoped system were retained. However, one would expect some change of these parameters on doping. Evidently, when further information on these changes becomes available it will be able to be incorporated in simulation work. An improved representation of interchain interactions and defects, including sp^3 carbons and covalent crosslinks is envisageable. The present work, combining molecular dynamics simulation with inelastic neutron scattering, can be considered as a first step towards the elucidation of the complex three-dimensional dynamics of doped, conjugated polymers.

ACKNOWLEDGMENTS

We thank Dr. Marc Gingold for computational assistance. Financial assistance is acknowledged from the Commissariat à l'Energie Atomique.

[1] *Proceedings International Congress on Synthetic Metals 1990*, [Synth. Met. **49** (1991)].
[2] H. Naarmann and N. Theophilou, Synth. Met. **22**, 1 (1987).
[3] A. J. Heeger, S. Kivelson, J. R. Schriefer, and W. P. Su, Rev. Mod. Phys. **60**, 781 (1988).
[4] A. J. Dianoux, in *Industry and Technological Applications of Neutrons*, in *Proceedings of the International School of Physics Enrico Fermi, CXIV*, edited by M. Fontana, F. Rusticelli, and R. Coppola (North–Holland, Amsterdam, 1992), pp. 15–47.
[5] G. R. Kneller, W. Doster, M. Settles, S. C. Cusack, and J. C. Smith, J. Chem. Phys. **97**, 8864 (1992).
[6] G. R. Kneller and A. Geiger, Mol. Phys. **70**, 465 (1990).
[7] J. C. Smith, S. Cusack, B. Tidor, and M. Karplus, J. Chem. Phys. **93**, 2974 (1990).
[8] A. J. Dianoux, G. R. Kneller, J.-L. Sauvajol, and J. C. Smith, J. Chem. Phys. **99**, 5586 (1993).
[9] J. L Sauvajol, D. Djurado, A. J. Dianoux, N. Theophilou, and J. E. Fischer, Phys. Rev. B **43**, 14 305 (1991). The frequency of the lowest-frequency $G_{\|}$ feature was wrongly cited as being 2.9 meV in this article. The correct frequency is 1.5 meV.
[10] J. L. Sauvajol, D. Djurado, A. J. Dianoux, and J. E. Fischer, J. Chim. Phys. (Paris) **89**, 969 (1992).
[11] J. L. Sauvajol, A. J. Dianoux, P. Papanek, C. Mathis, and J. E. Fisher (in preparation).
[12] B. Brooks, R. Bruccoleri, B. Olafson, D. States, S. Swaminathan, and M. Karplus, J. Comput. Chem. **4**, 187 (1983).
[13] W.-P. Su, J. R. Schreiffer, and A. J. Heeger, Phys. Rev. Lett. **42**, 1698 (1979).
[14] W.-P. Su, J. R. Schreiffer, and A. J. Heeger, Phys. Rev. B **22**, 2099 (1980).

[15] D. K. Campbell, T. A. DeGrand, and S. Mazumdar, Phys. Rev. Lett. **52**, 1717 (1984).
[16] P. Tavan and K. Schulten, Phys. Rev. B **38**, 433 (1987).
[17] S. Mazumdar and D. K. Campbell, Phys. Rev. Lett. **55**, 2067 (1985).
[18] J. F. Rabolt, T. C. Clarke, and G. B. Street, J. Chem. Phys. **71**, 4614 (1979).
[19] C. Benoit, O. Bernard, M. Palpacuer, M. Rolland, and M. J. M. Abadic, J. Phys. (Paris) **44**, 1307 (1983).
[20] X. Q. Yang, D. B. Tanner, M. J. Rice, H. W. Gibson, A. Feldblum, and A. J. Epstein, Solid State Commun. **61**, 335 (1987).
[21] B. Roux, Ph.D. thesis, Harvard University, 1990.
[22] P. Bernier, C. Fite, A. El-Khodany, F. Rachdi, K. Zruber, H. Bleier, and N. Coustel, Synth. Met. **37**, 41 (19XX).
[23] W. Winokur, Y. B. Moon, A. J. Heeger, J. Barker, D. C. Bott, and H. Shirakawa, Phys. Rev. Lett. **58**, 2329 (1987).
[24] R. H. Baughman, N. S. Murthy, H. Eckhardt, and M. Kertesz, Phys. Rev. B **46**, 10515 (1992).
[25] P. W. Carter and J. D. Porter, Phys. Rev. B **43**, 14 478 (1991).
[26] W. Winokur, Y. B. Moon, A. J. Heeger, J. Barker, and J. Orenstein, Phys. Rev. Lett. **58**, 2329 (1987).
[27] J. P. Ryckaert, Mol. Phys. **55**, 549 (1985).
[28] G. Sesé, C. R. A. Catlow, and B. Vessal, Mol. Simul. **9**, 99 (1992).
[29] G. Sesé and C. R. A. Catlow, Philos. Mag. B **68**, 397 (1993).
[30] G. R. Kneller, Mol. Simul. **7**, 113 (1991).
[31] Q. Zhu, J. E. Fischer, R. Zuzik, and S. Roth, Solid State Commun. **83**, 179 (1992).
[32] R. H. Baughman, S. L. Hsu, L. R. Anderson, G. P. Pez, and A. Signorelli, in *Molecular Models, NATO Conference Series*, edited by W. E. Hatfield (Plenum, New York, 1979), pp. 187–201.
[33] C. R. Fincher, C.-E. Chen, A. J. Heeger, A. G. MacDairmid, and J. B. Hastings, Phys. Rev. Lett. **48**, 100 (1982).
[34] A. J. Dianoux, G. R. Kneller, J.-L. Sauvajol, and J. C. Smith, J. Noncryst. Solids (in press).
[35] K. D. Moeller, G. P. Williams, C. Hirschmugl, S. Steinhauser, and J. C. Smith, Biophys. J. **61**, 276 (1992).
[36] V. A. Kuprievich, Phys. Rev. B **40**, 3882 (1989).
[37] S. Kivelson, W. P. Su, J. R. Schreiffer, and A. J. Heeger, Phys. Rev. Lett. **58**, 1899 (1987).
[38] S. Xie, L. Mei, and X. Sun, Phys. Rev. B **46**, 6169 (1992).
[39] A. Girlando, A. Painelli, and Z. G. Zoos, J. Chem. Phys. **98**, 7459 (1993).
[40] D. Emin, Phys. Rev. B **33**, 3973 (1986).
[41] H. A. Mizes and E. M. Conwell, Phys. Rev. Lett. **70**, 1505 (1993).
[42] Y. N. Gartstein and A. A. Zakhidov, Solid State Commun. **60**, 105 (1986).
[43] M. J. Field, J. Phys. Chem. **95**, 5104 (1991).